Supporting Information

Green *in Situ* Growth Solid Electrolyte Interphase Layer with High Rebound Resilience for Long-life Lithium Metal Anodes

Na Wu,[*,†] *Ya-Ru Shi,*[†] *Ting Jia,* [†] *Xue-Ning Du,* [†] *Ya-Xia Yin,* [‡] *Sen Xin,*[*,‡] *and Yu-Guo Guo,*[*,‡]

†Key Laboratory of Inorganic Nanomaterials of Hebei Province, College of Chemistry and Material Science, Hebei Normal University, Shijiazhuang 050024, P. R. China

‡CAS Key Laboratory of Molecular Nanostructure and Nanotechnology, CAS Research/ Education Center for Excellence in Molecular Sciences, Beijing National Laboratory for Molecular Sciences (BNLMs), Institute of Chemistry, Chinese Academy of Sciences (CAS), Beijing 100190, P. R. China

Corresponding Author

*E-mail: willywu@hebtu.edu.cn.

*E-mail: xinsen08@iccas.ac.cn.

*E-mail: ygguo@iccas.ac.cn.

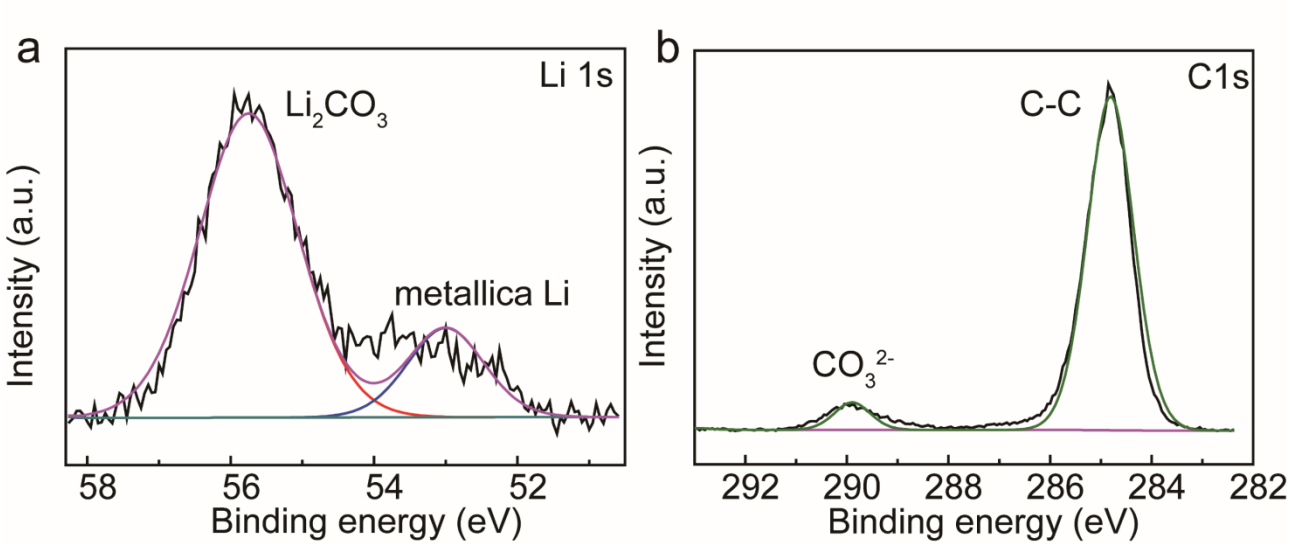

Figure S1. The XPS results of bare Li anode. C1s spectra a) and Li 1s spectra b) of the bare Li in the pristine state.

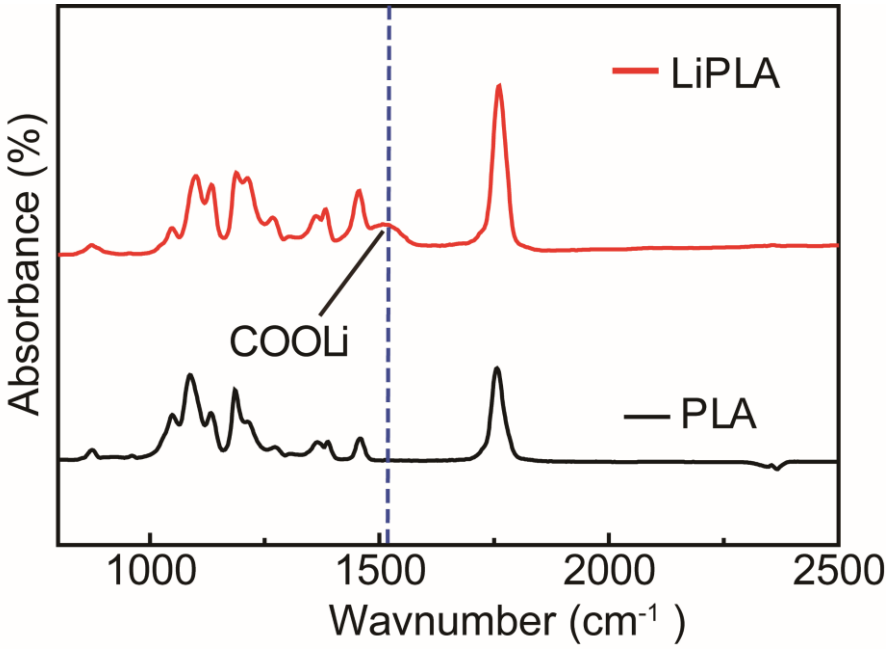

Figure S2. The fourier transform infrared spectroscopy of PLA and the LiPLA-Li anodes.

As shown in the FTIR (Figure S2), in comparison with the PLA, the organic group COO-Li emerge in the LiPLA-Li anodes, which further indicated that the LiPLA was generated via *in situ* reaction.

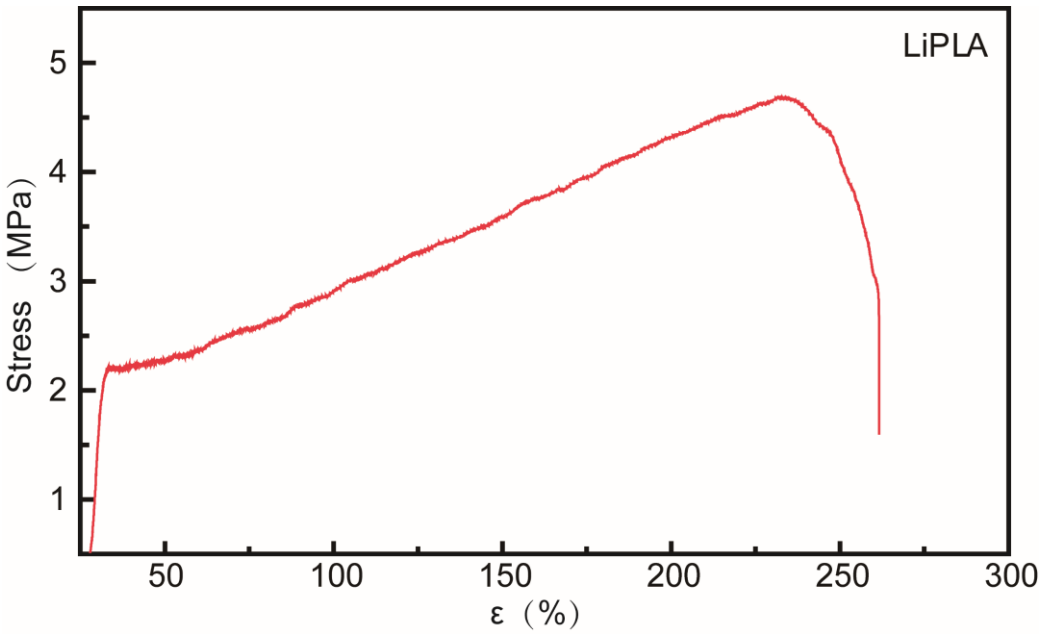

Figure S3. The stretch strain curve of LiPLA.

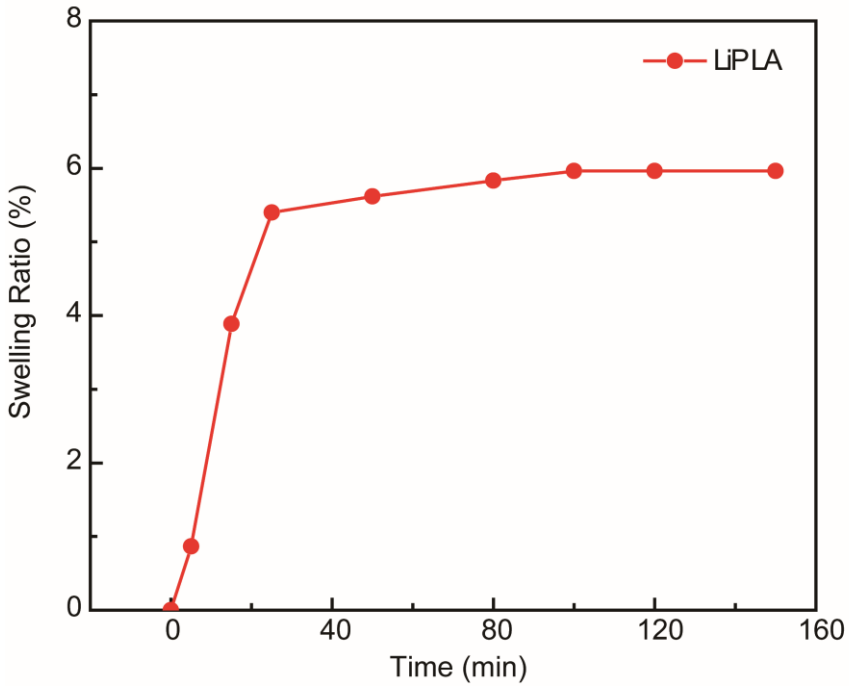

Figure S4. The swelling ratio of the LiPLA in the eletrolyte.

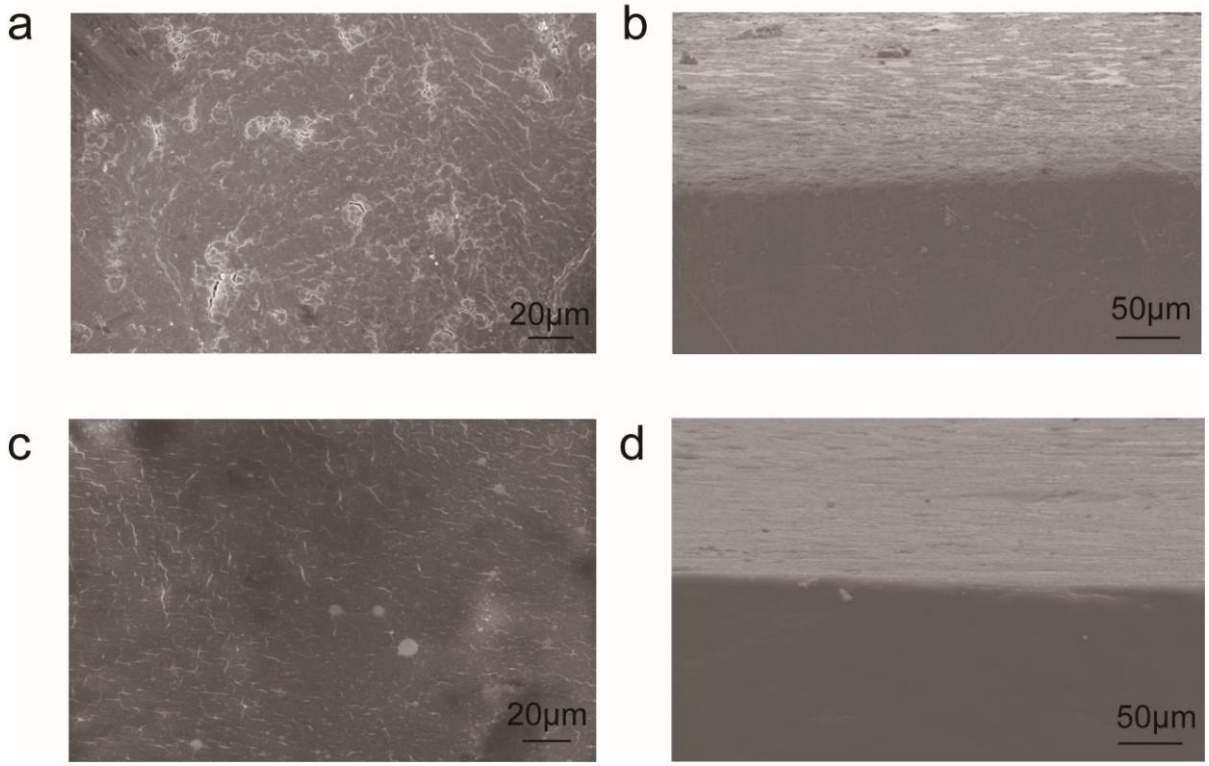

Figure S5. a) The top view and b) the side view SEM images of the pristine Li anodes after 11 cycles. c) The top view d) and the side view SEM images of LiPLA-Li anodes after 11 cycles (Current density : 0.5mA cm^{-2}, Capacity:1mA h cm^{-2}).

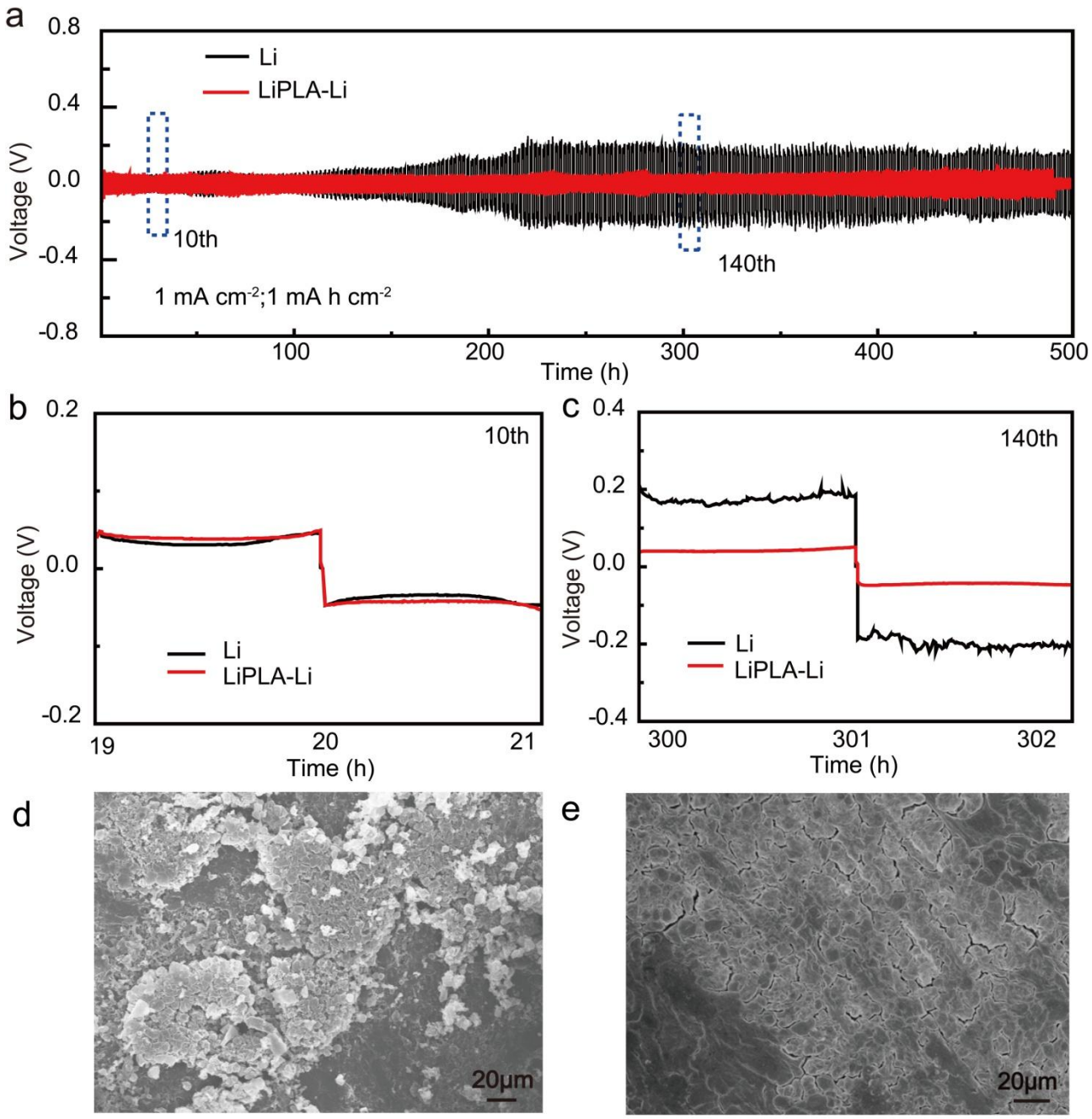

Figure S6. a) The comparison of cycling stability of the symmetric Li/Li cells with the pristine Li anodes and the LiPLA-Li anodes. Detailed voltage profiles for: b) 10th, c) 140th cycles. The top view SEM images of d) the pristine Li anodes and e) the LiPLA-Li anodes after 300 h in the symmetric Li/Li cells (Current density: 1mA cm^{-2}, Capacity: 1mA h cm^{-2}).

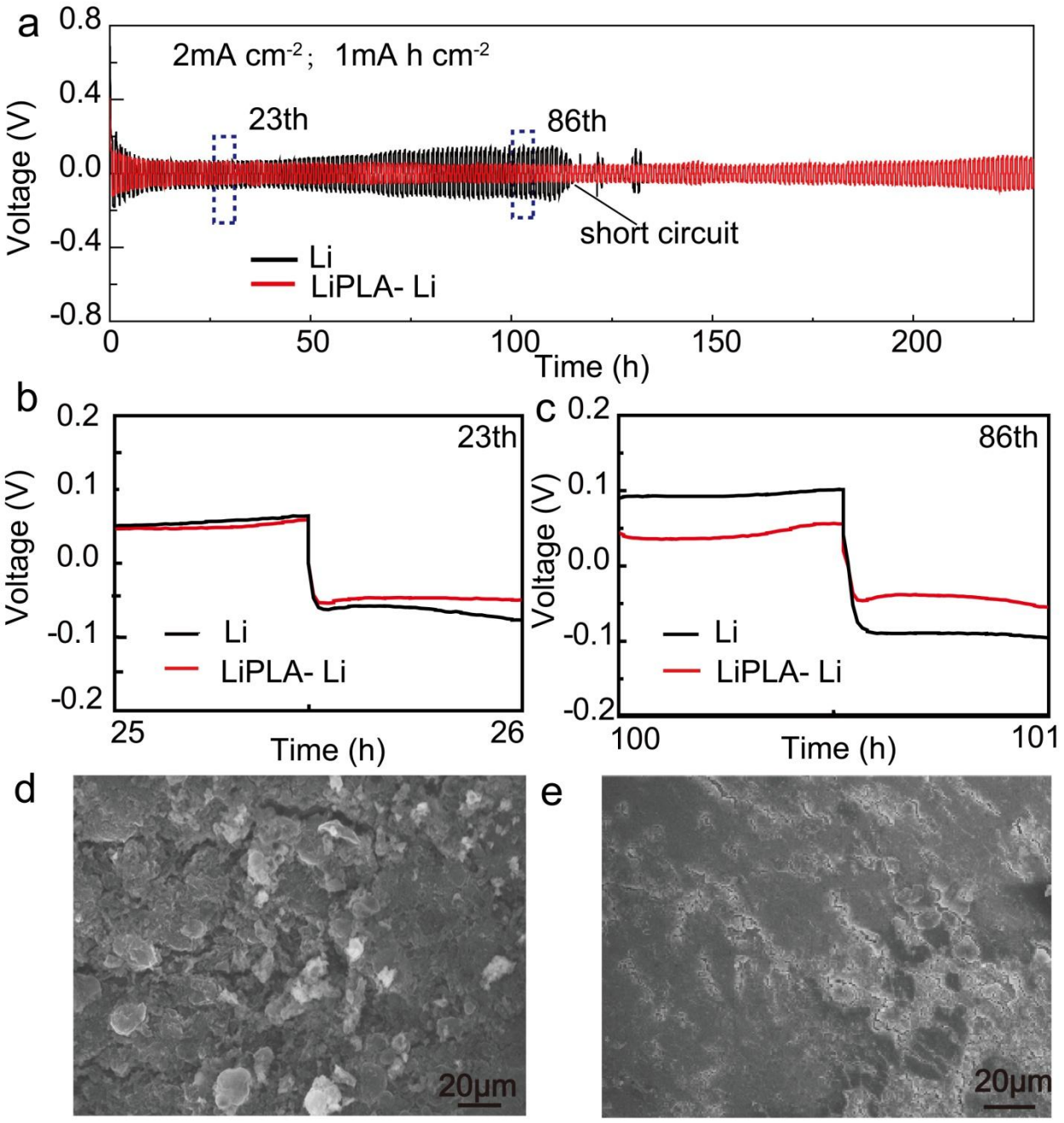

Figure S7. a) The comparison of cycling stability of the symmetric Li/Li cells with the pristine Li and the LiPLA-Li anodes. Detailed voltage profiles for: b) 23th, c) 86th cycles. The top view SEM images of d) the pristine Li anodes and e) the LiPLA-Li anodes after cycling 100 h in the symmetric Li/Li cells (Current density : 2mA cm^{-2}, capacity:1mA h cm^{-2}).

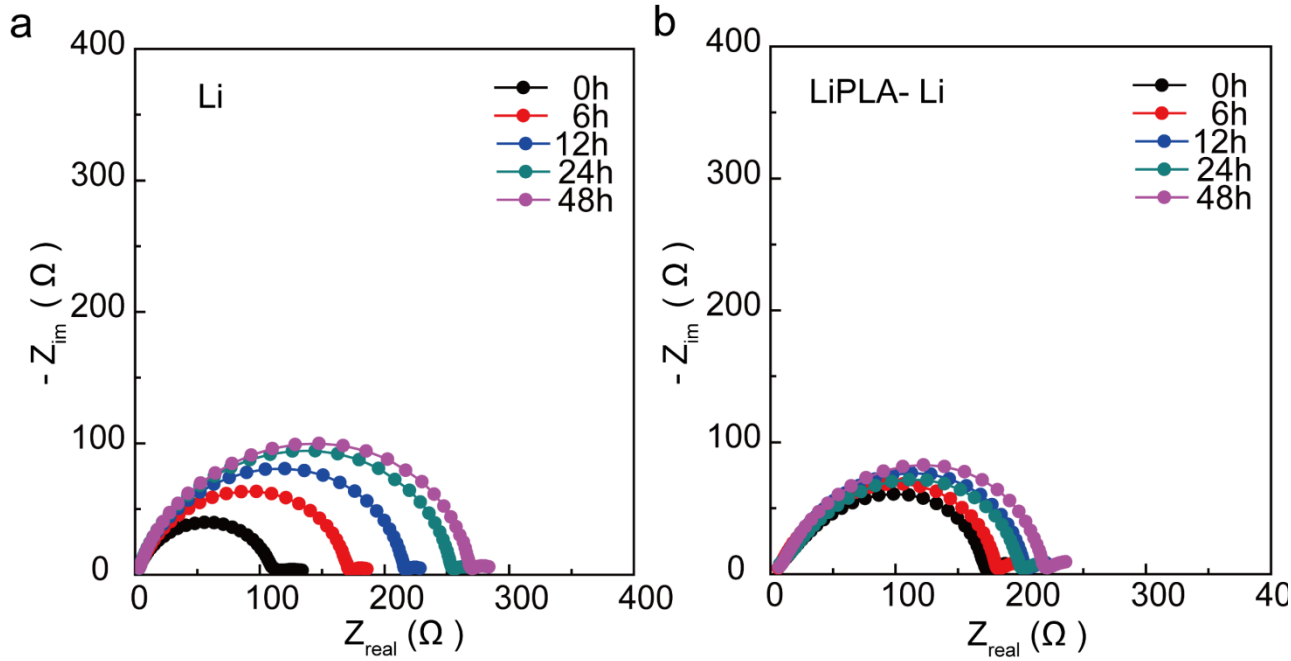

Figure S8. EIS plots of the symmetric Li-Li cells with a) the pristine Li anodes and b) the LiPLA-Li anodes after different standing time.

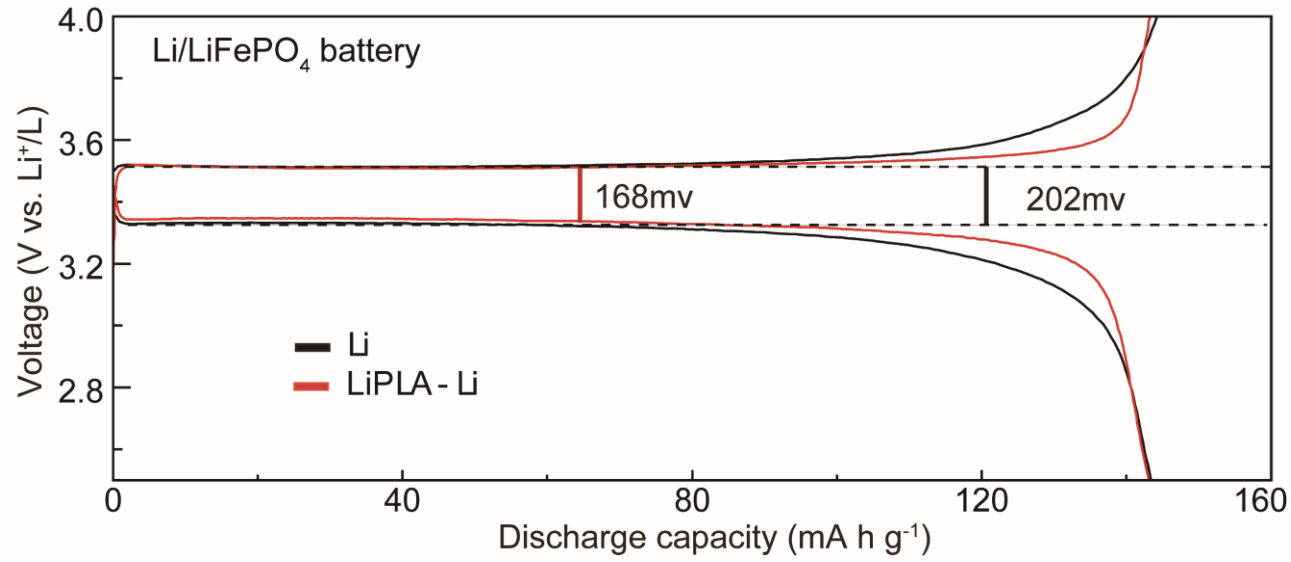

Figure S9. The typical charge/discharge profiles of Li/$LiFePO_4$ batteries with the pristine Li anodes and the LiPLA-Li anodes after activation at 0.5 C.

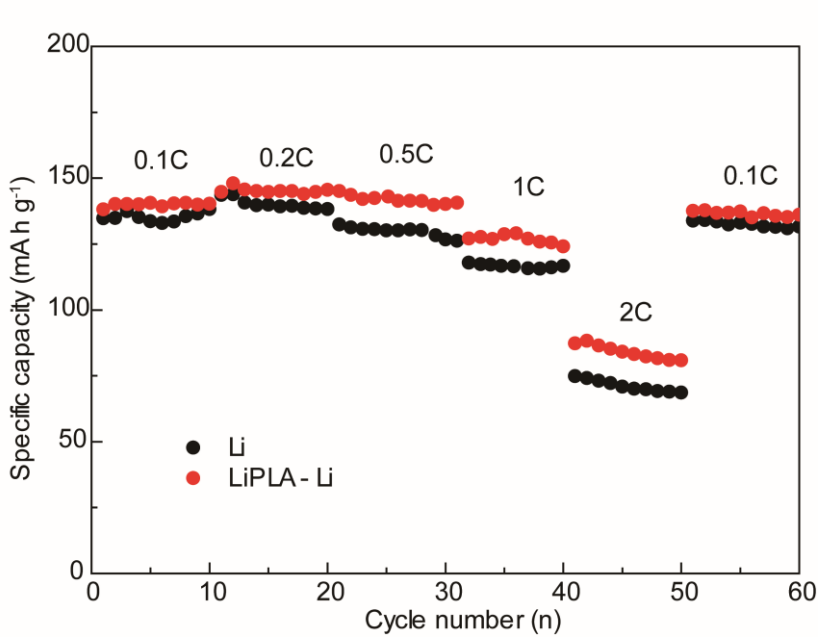

Figure S10. Rate capabilities of the Li/$LiFePO_4$ batteries with the bare Li anode and the LiPLA-Li anode.

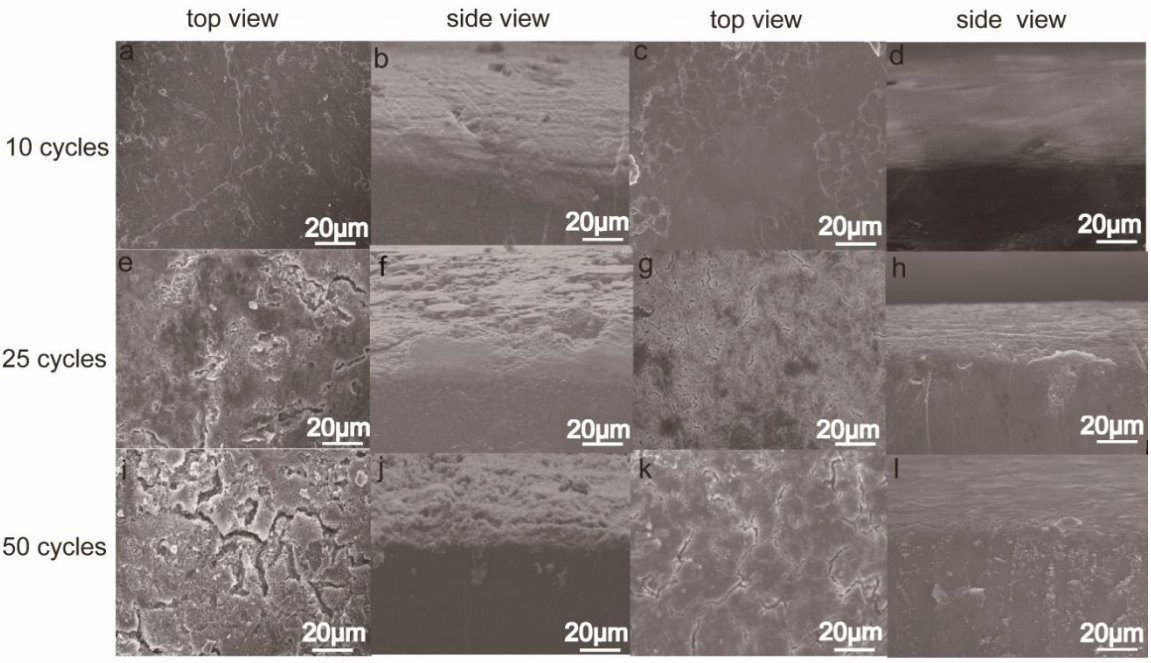

Figure S11. The top view images of a,e,i) the pristine Li anodes and c,g,k) the LiPLA-Li anodes and the side-view images of b,f,j) the pristine Li and d,h,j) the LiPLA-Li respectively after different cycles in the Li/$LiFePO_4$ batteries.

The Li/$LiFePO_4$ batteries with pristine Li and LiPLA-Li anodes after different cycles were disassembled to observe the morphology of Li metal anodes after cycling. With the charge/discharge process proceeding, the cracks of Li metal surface gradually increase, extending from partial to overall surface, and accompanied by fluffy Li dendrites (Figure S9a,b,e,f,i,j). The results indicate that the Li ion deposition is uneven. However, the surface of the anodes with PLALi is appeared a small amount of cracks in the cycling process, almost no lithium dendrites and the surface of Li metal are smooth (Figure S8c,d,g,h,k,l), corresponding to the resultes in the Li/Li systemtic cells. These phenomeon imply that the LiPLA has a positive impact to the interfacial stability.

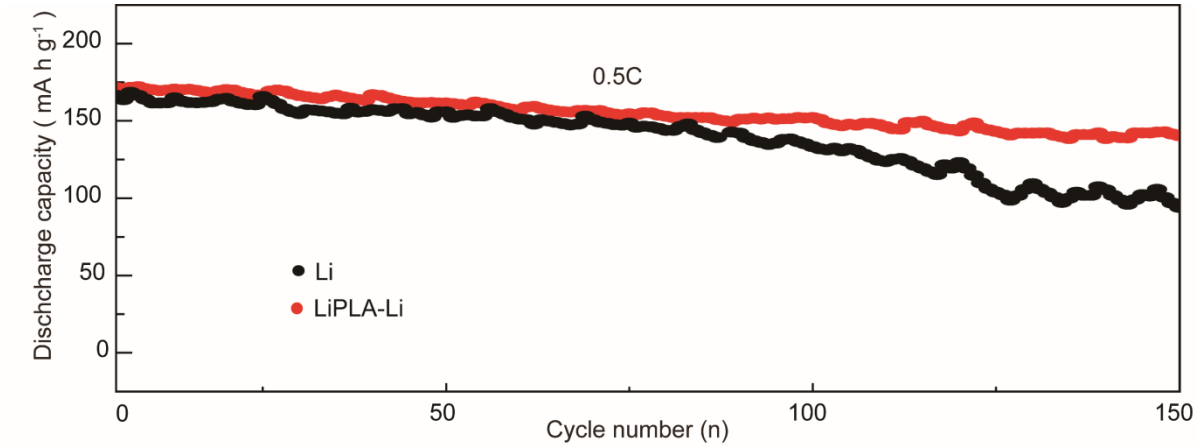

Figure S12. Cycling performance of the Li/$LiNi_{3/5}Co_{1/5}Mn_{1/5}O_2$ batteries using pristine Li and LiPLA-Li anodes at 0.5 C.

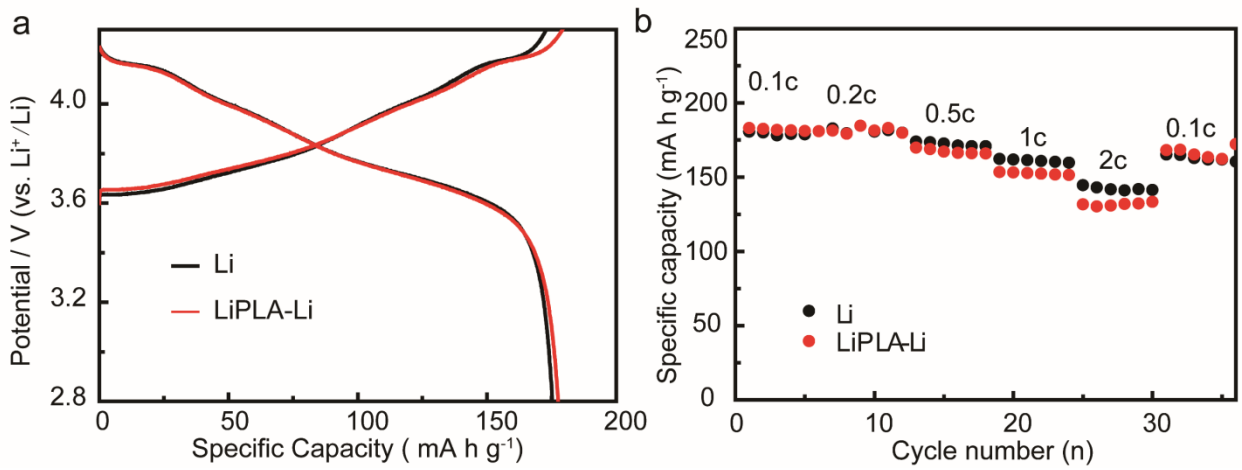

Figure S13. a) Initial charge and discharge profiles of the Li/$LiNi_{3/5}Co_{1/5}Mn_{1/5}O_2$ batteries with the two anodes at 0.1C. b) Rate capabilities of the Li/$LiNi_{3/5}Co_{1/5}Mn_{1/5}O_2$ batteries with the two anodes. All the experiments were conducted in the voltage range of 2.8-4.3V *vs* Li^+/Li at room temperature.

When measured at different current density, the $LiFePO_4$ full batteries with LiPLA-Li anode delivers higher reversible capacity and better recoverability than the one with bare Li (Figure S10). Furthermore the similar rate capability in $LiNi_{3/5}Co_{1/5}Mn_{1/5}O_2$ battery with bare Li and LiPLA-Li anode (Figure S13b) reveals that the LiPLA protective layer has little impact on the dynamics of the batteries.

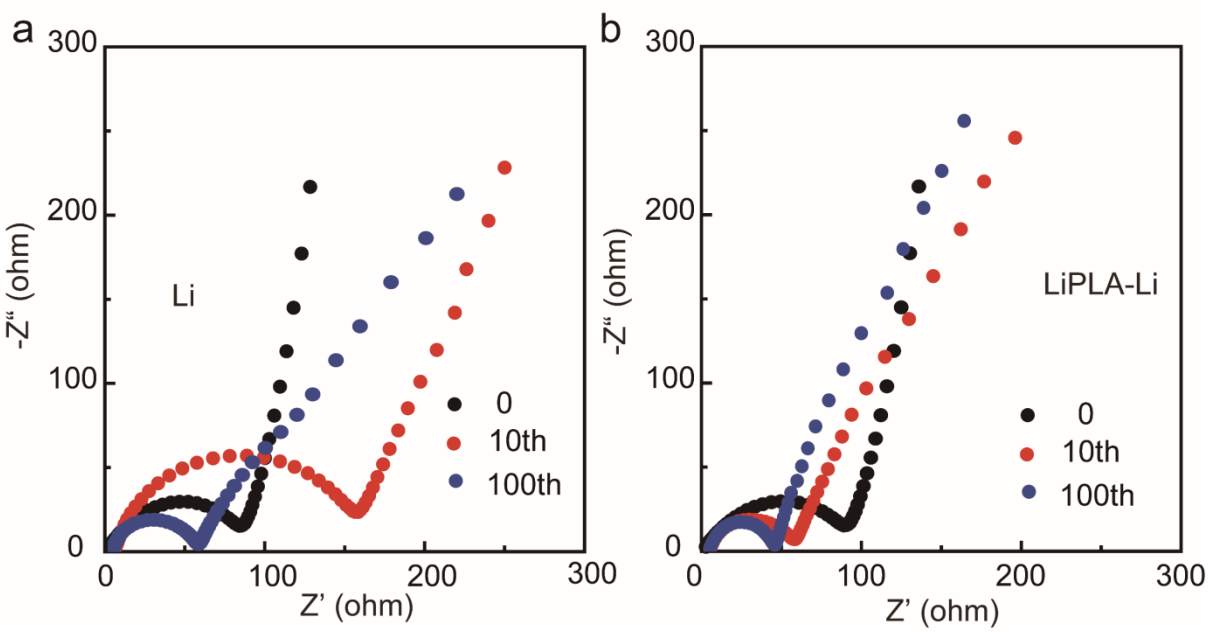

Figure S14. The EIS plots of the Li/$LiNi_{3/5}Co_{1/5}Mn_{1/5}O_2$ batteries with a) the prostine Li and b) the LiPLA anodes after the 0, the 10th and the 100th cycles.